Project Report
Of the Minor Research Project 2012-14
Funded by UGC Western Regional Office Pune

"Preparation, Characterization and Magnetization Studies of Some Soft Ultrafine Mixed Metal Ferrites"

Principal Investigator
Dr. Vikas J. Pissurlekar

Co- Investigator
Prof. Jayant S. Budkuley

Department of Chemistry
P. E. S's Ravi S. Naik College of Arts & Science
Farmagudi Ponda
Goa- 403401.

Acknowledgements

Dr. Vikas J. Pissurlekar, Principal Investigator wishes to express sincere gratitude to U.G.C. Western Regional office Pune for sanctioning a Minor Research Project entitled "Preparation, Characterization and Magnetization Studies of Some Soft Ultrafine Mixed Metal Ferrites".

My sincere thanks to my mentor, guide and PhD supervisor Professor Jayant S. Budkuley, Retired Professor and Head of the Department of Chemistry of Goa University for encouraging and motivating me to work on this project topic and for continuous support and guidance during the project.

I am also thankful to the Management of Ponda Education Society for their support and encouragement throughout the project.

I would like to thank Dr. A. S. Dinge, Principal of P. E. S's Ravi S. Naik College of Arts & Science Farmagudi Ponda Goa for his support, and also for providing all the necessary facilities to carry out the project work

I would also like to thank my B.Sc. students who carried out the experimental work as their project work. Mr. Pranav Naik for providing some of the instrumental data. The Head, Department of Physics, Goa University and various other institutions like NCAOR and ADEC Technologies Goa, for helping in gathering the various instrumental data for the samples of the project work,

The principal investigator is thankful to the Librarian of P. E. S's Ravi S. Naik College of Arts & Science and Goa University for providing library facilities.

I would also like to acknowledge the cooperation of Shri. R.V. S. Kuncolienkar the accountant of the college and other administrative staff and my departmental colleagues especially Mr. Nitin Naik, Mrs. Swarupa Kerkar, Mr. Ranganath Naik, Mr.Prakash Naik, Mr.Eknath Naik and Mr. Raju Bandodkar.

Lastly, I would like to thank all my colleagues, family and friends for their support in various capacities during the course of the present study.

- Dr. Vikas J. Pissurlekar

Content

page No

CHAPTER I

LITERATURE SURVEY

I.1 Introduction

What is Ferrite?

Ferrites are categorized as electro-ceramics with ferromagnetic properties. They are ceramic like material with iron (III) oxide (Fe_2O_3) as their principal component. Ferrite exhibits ferrimagnetism due to the super-exchange interaction between electrons of metal and oxygen ions. The opposite spins in ferrite results in the lowering of magnetization compared to ferromagnetic metals where the spins are parallel. Due to the intrinsic atomic level interaction between oxygen and metal ions, ferrite has higher resistivity compared to ferromagnetic metals. This enables the ferrite to find applications at higher frequencies and makes it technologically very valuable.

The chemical formula of ferrite is generally expressed as $MeFe_2O_4$, where 'Me' represents a divalent metal ion. (e.g. Fe^{2+}, Ni^{2+}, Mn^{2+}, Mg^{2+}, Co^{2+}, Zn^{2+}, Cu^{2+} etc). The crystal lattice of ferrite is spinel. Most important commercial derivatives of these ferrites are Zn^{2+} substituted Ni and Mn ferrite represented as $NiZnFe_2O_4$ and $MnZnFe_2O_4$ respectively. The major difference among these two ferrites is in their resistivity.

The magnetic property of ferrite is the manifestation nature of ions and their relative lattice position. Ferrites exist in spinel lattice structures. Metal ions are located at octahedral and tetrahedral positions. Fe^{2+}, Ni^{2+}, Mn^{2+} etc ions prefer tetrahedral sites. Ni-Zn ferrite and Mn-Zn ferrites has inverse spinel structures where a part of the B atom occupies in the tetrahedral site and A atom occupy the Octahedral site. Depending on the composition and process conditions such as sintering temperature and atmosphere, the lattice site occupancy changes leading to the change in magnetic and electrical properties. This shows that in ferrite manufacturing both composition and process conditions are very critical to get the required quality

Ferrites exhibits ferrimagnetism. This means there is net magnetic moment in molecular level as a result of electronic interaction between metal and oxygen ions called super exchange. In bulk ferrite, there are domains called Weiss Domains in which all these molecular magnets

are aligned in one direction. Domain walls separates different domain aligned in random directions and in the presence of an external magnetic field these moments can be forced to align in one direction. Some energy has to be spent for this process and the magnetization always lags behind the magnetizing field and results in a magnetization loop. This is called as B-H Loop.

The term ferrimagnetism was coined by the French physicist Louis Neel, who first studied ferrites systematically on the atomic level. There are several types of ferrimagnetism. In collinear ferrimagnetism the fields are aligned in opposite directions, in triangular ferrimagnetism the field orientation may be at various angles to each other. Ferrites can have several different types of crystalline structures, including spinel, garnet, perovskite, and hexagonal.

The most important properties of ferrites include high magnetic permeability and high electrical resistance. High permeability to magnetic fields is particularly desirable in devices such as antennas. High resistance to electricity is desirable in the cores of transformers to reduce eddy currents. Ferrites of a type known as square-loop ferrites can be magnetized in either of two directions by an electric current. This property makes them useful; in the memory cores of digital computers, since it enables a tiny ferrite ring to store binary bits of information. Another type pf computer memory can be made of certain single crystal ferrites in which tiny magnetic domains called bubbles can be individually manipulated. A number of ferrites absorb microwave energy in only one direction or orientation; for this reason, they are used in microwave wave guides.

1.2. CLASSIFICATION OF FERRITES:-

Ferrite magnets, or ferromagnetic materials, are classified broadly on the basis of a property called magnetic coercivity, or perseverance of internal magnetism and structure.

1.2.1. SOFT FERRITES:

Soft ferrites are extensively used in electronic devices because of their good magnetic properties. The most important property of soft ferrites is their high magnetic polarization in combination with a high electrical resistivity much higher than that of metallic magnetic materials. The most important soft ferrite material is Manganese Zinc Ferrite ($MnZnFe_2O_4$).

Soft ferrites are also used in transformer or electromagnetic cores contain nickel, zinc, or manganese compounds. They have a low coercivity which means that the materials magnetization can easily reverse direction without dissipating much energy (hysteresis losses), while the materials high resistivity prevents eddy currents in the core, another source of energy loss. Because of their comparatively low losses at high frequencies, they are extensively used in the cores of RF transformers and inductors in applications such as Switched-mode power supplies.

The most common soft ferrites are:

- Manganese-Zinc ferrite (Mn-Zn, with the formula $Mn_xZn_{(1-x)}Fe_2O_4$. Mn-Zn ferrites have higher permeability and saturation induction in comparison than Ni-Zn.
- Nickel-Zinc ferrite (Ni-Zn, with the formula $Ni_xZn_{(1-x)}Fe_2o_4$. Ni-Zn ferrites exhibit higher resistivity than Mn-Zn, and are therefore more suitable for frequencies above 1MHz.

1.2.2 . HARD FERRITES:

In contrast, permanent ferrites magnets are made of hard ferrites, which have a high coercivity and high remanence after magnetization. These are composed of iron and barium or strontium oxides. The high coercivity means the materials are very resistant to becoming demagnetized, an essential characteristic for a permanent magnet. They also conduct magnetic flux well and have a high magnetic permeability; this enables these so-called ceramic magnets to store stronger magnetic fields than iron itself. They are cheap, and are widely used in household products such as refrigerator magnets. The maximum magnetic field B is about 0.35tesla and the magnetic field strength H is about 30 to 160 kilo ampere turns per meter (400 to 2000 oersteds). The density of ferrite magnets is about $5g/cm^{3.}$

The most common hard ferrites are:

- Strontium ferrite, $SrFe_{12}O_{19}$ ($SrO.6Fe_2O_3$), a common material for permanent magnet applications.
- Barium ferrite, $BaFe_{12}O_{19}$ ($BaO.6Fe_2O_3$), a common material for permanent magnet applications. Barium ferrites are ceramics that are generally stable to moisture and

corrosion- resistant. They are used in e.g. subwoofer magnets and as a medium for magnetic recording, e.g. on magnetic stripe cards.

- Cobalt ferrite, $CoFe_2O_4$ ($CoO.Fe_2O_3$), used in some media for magnetic recording.

1.2.3. FERROSPINELS:

- Normal ferrites in which all the 'Me' ion are in the tetrahedral A sites and all the Fe^{3+} ions are in the octahedral sites.
- Inverse ferrites, in which all the 'Me' ions and half of the Fe^{3+} ions are in B sites, while remaining Fe^{3+} ions are in A sites.
- Random ferrites in which the 'Me' and Fe^{3+} are distributes uniformly over tetrahedral and octahedral sites.
- The magnetic interaction between the magnetic ions in spinels is of indirect type (super exchange), i.e. it takes place via the intermediate oxygen ions.
- In a spinel structure, each oxygen ion is surrounded by three B cations and one A cation.

1.2.4. Garnets:

The garnet mineral known as YIG, chemical formula for the ferrogarnets is '$Me_3Fe_5O_{12}$' and 'Me' is a trivalent ion such as a rare earth of Y^{3+}, containing the rare-earth element yttrium, has formula $Y_3Fe_5O_{12}$; it is used in microwave circuitry. The unit cell is cubic and contains eight metal ions are distributed over three types of sites. The 'Me' ions occupy the dodecahedral (called C sites) where they are surrounded by eight oxygen ions; whereas the Fe^{3+} ions are distributed over tetrahedral and octahedral sites in the ratio 3:2. Thus the cation distribution is $Mec_3Fea_2Fed_3O_{12}$.

1.2.5. Orthoferrites:

Orthoferrites have the general formula '$MeFeO_3$'; where 'Me' is a large trivalent metal ion, such as rare earth ions as Y. they crystallize in a distorted perovskite structure with an orthorhombic unit cell. The rare-earth ion subsystem acquires magnetization due to an interaction with the iron subsystem. The ortho-ferrites are particularly interesting because of the presence of an anti systematic exchange interaction which involves the vector across product of neighboring spins as opposed to the usual scalar product. In the absence of this interaction, the ortho ferrite would be antiferromagnetic. Its presence leads to a small canting

of the sub-lattices, making the ortho-ferrite "weak" ferromagnetic. Another interesting feature of these materials is the fact that some of them exhibit a transition as a function of temperature, in which the direction of the antiferromagnetically ordered spins and consequently also of the net magnetization rotates by 90^0.

Examples:

- Lanthanum orthoferrite, $LaFeO_3$
- Dysprosium ortho ferrite, $DyFeO_3$

1.2.6. Hexagonal ferrites:

There are number of ferrites that crystallize in hexagonal structure and some of them have gained considered technological importance in recent years. These ferrites are further sub-classifies into M, W, Y, Z and U compounds. The 'M 'has the simplest structure. Since their discovery in the 1950s there has been an increasing degree of interest in the hexagonal ferrites, also known as hexa-ferrites, which is still growing exponentially today. These have been massively important materials commercially and technologically accounting for the bulk of the total magnetic materials manufactured globally, and they have a multitude of uses and applications. As well as their use as permanent magnets, common applications are as magnetic recording and data storage materials, and as components in electrical devices, particularly those operating at microwave/GHz frequencies.

Barium ferrites, the well-known hard ferrite belong to this class. The compound have the general formula' $MeFe_{12}O_{19}$' where 'Me' is a divalent ions of a large ionic radius, such as Ba^{2+}, Sr^{2+} or Pb^{2+}. In these one iron per formula unit is present as Fe^{2+} to allow for the charge compensation.

M- type ferrites, such as $BaFe_{12}0_{19}$ (bam or barium ferrite), $SrFe_{12}O_{19}$ (SrM or strontium ferrite) , and cobalt-titanium substituted M ferrite, Sr or $BaFe_{12-2x}Co_xTi_xO_{19}$ (CoTiM).

Z-type ferrites ($Ba_3Me_2Fe_{24}O_{41}$) such as $Ba_3Co_2Fe_{24}O_{41}$, or Co_2Z.

Y-type ferrites ($Ba_2Me_2Fe_{12}0_{22}$), such as $Ba_2Co_2Fe_{12}O_{22}$, or Co_2Y.

W-type ferrites ($BaMe_2Fe_{16}0_{27}$), such as $BaCo_2Fe_{16}0_{27}$, or CO_2W.

X-type ferrites ($Ba_2Me_2Fe_{28}0_{46}$), such as $Ba_2Co_2Fe_{28}O_{46}$, or Co_2X.

U-type ferrites ($Ba_4Me_2Fe_{36}O_{60}$), such as $Ba_4Co_2Fe_{36}O_{60}$, or Co_2U.

The best known hexagonal ferrites are those containing barium and cobalt as divalent cations, but many variations of these and hexa-ferrites containing other cations (substituted or doped) will also be discussed, especially M, W, Z and Y ferrites containing strontium, zinc, nickel and magnesium. The hexagonal ferrites are all ferrimagnetic materials, and their magnetic properties are intrinsically linked to their crystalline structures. They all have a magneto-crystalline anisotropy (MCA) that is the induced magnetisation has a preferred orientation within the crystal structure.

1.3. Spinel structure:

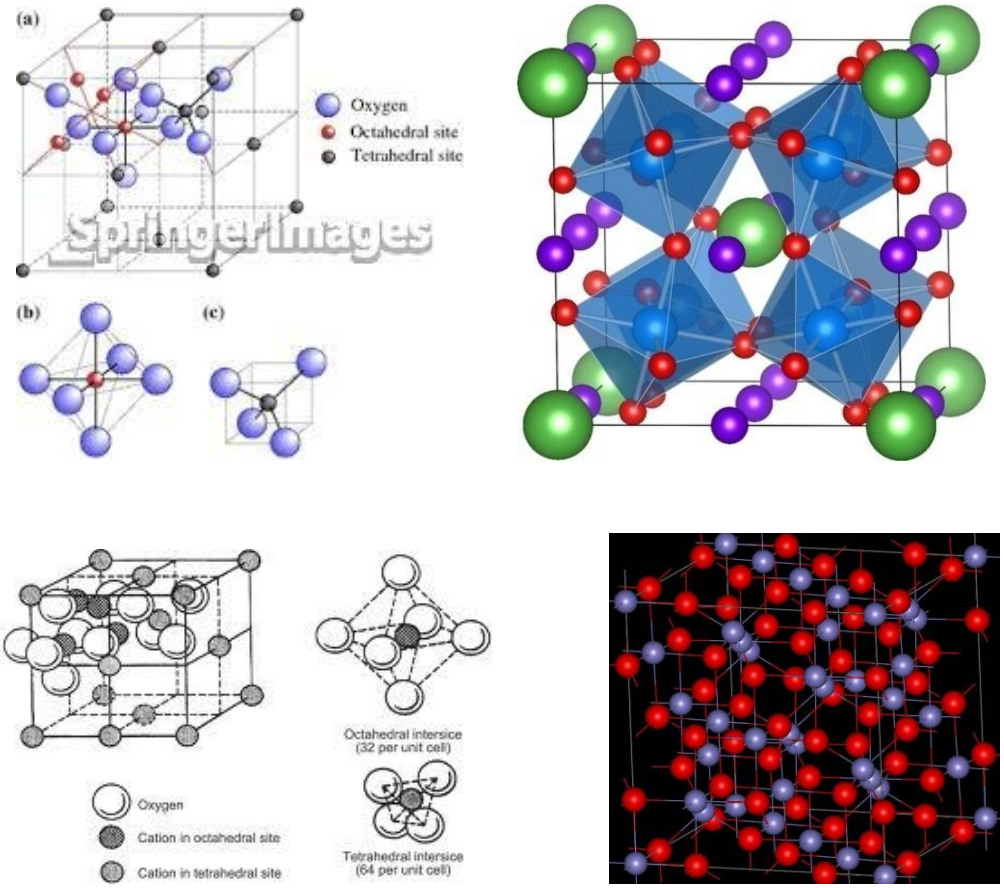

Fig: 1.1.: Spinel structure

The spinal ferrite structure MFe_20_4 can be described as a cubic close-packed arrangement of oxygen ions, with M^{2+} and Fe^{3+} ions at two different crystallographic sites. These sites have one octahedral and two tetrahedral sites per oxide. The tetrahedral points are smaller than the

octahedral points. B^{3+} ions occupy the octahedral holes because of a charge factor, but can only occupy half of the octahedral holes. A^{2+} ions occupy ⅛ of the tetrahedral holes.

The spinel has the general formula AB_2X_4, where:
A^{II} = a divalent cation like Mg, Cr, Mn, Fe, Co, Ni, Cu, Zn, Cd, Sn.
B^{III}= a trivalent cation like Al, Ga, In, Ti, V, Cr, Mn, Fe, Co, Ni.
X= O, S, Se etc.

In case of structure of normal spinels (AB_2O_4): The divalent A^{II} ions occupy tetrahedral voids, whereas the trivalent B^{III} ions occupy the octahedral voids in the closed packed arrangement of oxide ions.

A normal spine can be represented as : $(A^{II})^{tet}(B^{III})_2{}^{oct}O_4$. Eg. $MgAl_2O_4$ (known as spinel), Mn_3O_4, $ZnFe_2O_4$, $FeCr_2O_4$ (chromite) etc.

In case of structures of inverse spinels ($B(AB)O_4$): The A^{II} ions occupy the octahedral voids, whereas half of B^{III} ions occupy the tetrahedral voids. It can be represented as, $(B^{III})^{tet}(A^{II}B^{III})^{oct}O_4$. Eg. Fe_3O_4, (ferrite), $CoFe_2O_4$, $NiFe_2O_4$ etc.

The above inverse spinels can also be written as:
$Fe_2O_4= Fe^{III}(Fe^{II}Fe^{III})O_4$
$CoFe_2O_4= Fe^{III}(Co^{II}Fe^{III})O_4$
$NiFe_2O_4= Fe^{III}(Ni^{II}Fe^{III})O_4$

The number of octahedral sites occupied may be ordered or random. The random occupation leads to defected spinels. Eg. $NiAl_2O_4$ for which the formula can be written as $(Al_{0.75}Ni_{0.25})^{tet}(Ni_{0.75}Al_{1.25})^{octa}O_4$.

In order to explain the adoption of a particular cation distribution in a spinal structure, one must take into account the crystal field stabilization energies (CFSE) of the transition metals present. Some ions may have a distinct preference on the octahedral site which is dependent on the d-electron count. If the A^{2+} ions have a strong preference for the octahedral site, they

will force their way into it and displace half of the B^{3+} ions from the octahedral sites to the tetrahedral sites. If the B^{3+} ions have a low or zero octahedral site stabilization energy (OSSE), then they have no preference and will adopt the tetrahedral site.

Burdett and co-workers proposed an alternative treatment of the problem of spinel inversion, using the relative sizes of s and p atomic orbitals of the two types of atom to determine their site preference. This is because the dominant stabilizing interaction in the solids is not the crystal field stabilization energy generated by the interaction of the ligands with the d-electrons, but the σ-type interactions between the metal cations and the oxide anions. This rationale can explain anomalies in the spinel structures that crystal-field theory cannot, such as the marked preference of Al^{3+} cations for octahedral sites or of Zn^{2+} for tetrahedral sites using crystal field theory would predict that both have no site preference. Only in the cases where this size-based approach indicates no preference for one structure over another do crystal field effects make any difference – in effect they are just a small perturbation that can sometimes make a difference, but which often do not.

Nano particles are unique as important changes occur in the electronic band structure. The size dependent properties of material are very interesting not only to fabricate technologically important devices but also to understand how starting from atoms , molecules clusters evolve ending up in the solid and how the structure bonding , electronic structure and other properties changes during evolution. Magnetization in nano particles is considerably different from that of crystalline/polycrystalline material as they are characterized by a high value of surface to volume ratio with a large fraction of atoms present at grain boundaries. Magnetic materials possess some type of anisotropy which affects their magnetic behavior.

The most common method of preparation of ferrites is the conventional ceramic method; involving high temperature solid state reaction between constituent oxides or carbonates. The particles obtained are large and non-uniform in size, as well as non homogeneous on microscopic scale. The non-stoichiometry is due to extensive grinding and high heating temperature involved in preparation process and also due to possibility of presence of unreacted phases in the finished product. This also results in loss of fine particle size.

The chemical methods of preparation have advantages over conventional ceramic methods as it produces uniform, homogenous and with stoichiometric composition of the product. The demand for high performance of ferrite for especially for application requiring low loss at high frequencies has created the need for newer methods for preparing compositionally and structurally perfect ferrites exhibiting low magnetic and electrical losses.

There are different wet chemical methods such as co-precipitation, citrate precursor, sol gel etc.

Precursor methods are simple; inexpensive does not require much experimental set up and relatively fast. The ferrites obtained by this method are found to show better properties then those prepared by ceramic method.

The performance of ferrites depends on the synthesis process. It is also known that nano particles have physical dimensions in the range of few nanometers to less than a hundred nanometers.

1.4. Properties of ferrites:

1.4.1. Magnetic properties

Magnetic property depends upon concentration and non-magnetic ions in mixed ferrites. In case of Ni-Zn ferrites, Zn^{2+} are non-magnetic ions and Ni^{2+} are magnetically weak ions, therefore at lower concentration of Zn^{2+} ions, the saturation magnetization of mixed ferrites is high. Magnetic properties are most fundamental properties of any ferrite material. The magnetic properties include saturation magnetization, retentively, coercivity, permeability, susceptibility, and Curie temperature.

1.4.1. Saturation magnetization:

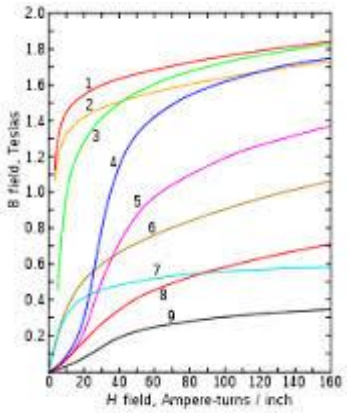

Fig: 1.2. Variation of magnetization against applied field.

Saturation is the state reached when an increase in applied external magnetic field H cannot increase the magnetization of the material further, so the total magnetic flux density B levels off. It is a characteristic particularly of ferromagnetic materials, such as iron, nickel, cobalt and their alloys. Saturation is most clearly seen in the magnetization curve (also called BH curve or hysteresis curve) of a substance, as a bending to the right of the curve. As the H field increases, the B field approaches a maximum value asymptotically, the saturation level for the substance. Technically, above saturation, the B field continues increasing, but at the paramagnetic rate, which is 3 orders of magnitude smaller than the ferromagnetic rate seen below saturation.

The relation between the magnetizing field H and the magnetic field B can also be expressed as the magnetic permeability:

$$\mu = B/H \text{ or the relative permeability}$$

$\mu_r = \mu/\mu_\circ$, where $\mu_\circ$ is the vacuum permeability. The permeability of ferromagnetic materials is not constant, but depends on H. In saturable material the relative permeability is not constant, but depends on H. In saturable materials the relative permeability increases with H to a maximum, then as it approaches saturation inverts and decreases toward one.

Different materials have different saturation levels. For example, high permeability iron alloys used in transformers reach magnetization saturation at 1.6 – 2.2 teslas (T), whereas

ferrites saturate at 0.2 – 0.5 T. some amorphous alloys saturate at 1.2 – 1.3 T. Mu metal saturates at around 0.8 T.

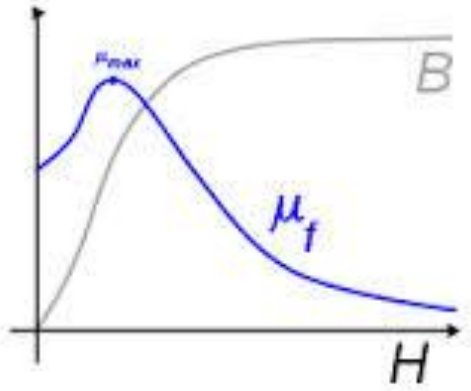

Fig:1.3. Variation of permeability.

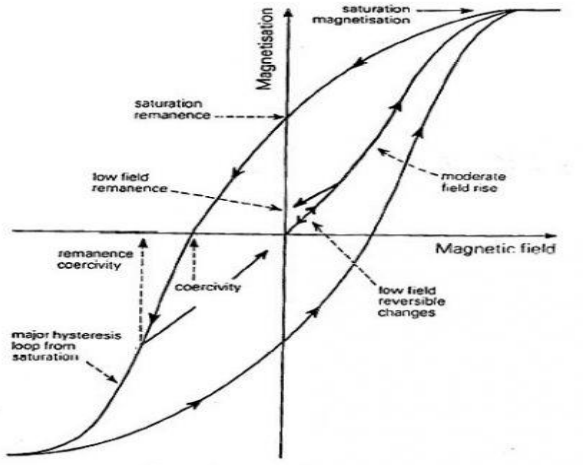

Fig: 1.4. The above diagram predicts Magnetization (M) versus Magnetic field strength (H)

The smooth curve depicts the rotation of the vector moment in the domain wall as the magnetic field strength (H) is varied. When the applied field is decreased magnetization is also decreased in multi domain bulk material, demagnetization occur primarily via spin rotation through the domain wall. If the demagnetization curve, during the removal of the applied field, does not allow the initial magnetization curve, the material displays hysteresis, which is the lag observed in the figure.

1.4.2. AC Susceptibility:

In electromagnetism, the magnetic susceptibility is a dimensionless proportionality constant that indicates the degree of magnetization of a material in response to an applied magnetic field. A related term is magnetizability, the proportion between magnetic moment and magnetic flux density [10]. A closely related parameter is the permeability which expresses the total magnetization of material and volume. When the magnetic susceptibility is measured in response to an AC magnetic field (i.e. a magnetic field that varies sinusoidally), this is called AC Susceptibility. AC Susceptibility (and closely related "AC Permeability") is complex quantities, and various phenomenons (such as resonances) can be seen in AC Susceptibility that cannot be seen in constant field (DC) Susceptibility. In particular, when the AC field is applied perpendicular to the detection direction (called the "transverse susceptibility" regardless of the frequency), the effect has a peak at the Ferromagnetic resonance frequency of the material with a given static applied field. Currently this effect is called the Microwave Permeability or Network Ferromagnetic Resonance in the literature. These results are sensitive to domain wall configuration of the materials and Eddy currents. In terms of ferromagnetic resonance, the effect of an AC field applied along the direction of magnetization is called Parallel Pumping.

1.4.3. Electrical properties:

Some of the important electrical properties of ferrites are resistivity, dielectric constant, etc.

1.4.3.1 Resistivity:

Ferrites have resistivity ranging from 10^3 to 10^{11} Ohms at room temperature. These wide ranges in resistivities of ferrites are explained on the basis of actual location of cations in the spinels structure and hopping mechanism. Their high conductivity is due to presence of ferrous and ferric ions in the crystallographically equivalent sites. The high resistivity in ferrites is associated with the occupation of B sites by other divalent metal ion and trivalent Fe ions. Thus spinel ferrites contain large number of oxygen ions and small number of metal ions in the interstitial spaces. Both Fe^{2+} and Fe^{3+} ions are at B sites, conduction takes place when electrons moves from Fe^{2+} and Fe^{3+} ions. The resistivity of ferrites is affected by temperature. The diffusion of charge carries from one state to other is to raise to photons and electrons hop between the possible only when the energy exceeds activation energy. The

thermal lattice vibrations consistently give pairs of state either by absorption or by emission of photons each time. In this way transport of charge carriers is achieved by hoping process through interaction with photons. On the basis of this the temperature dependence of resistivity of ferrites is given by the relation:

$$\rho=\rho_o \exp(-\Delta E/KT) \qquad 1.1$$

Where,

ρ_0= Temperature dependent constant

ΔE= Activation energy

K= Boltzmann constant

T= Absolute temperature

These factors which differentiate the electrical behavior, of the ferrite, from that of semiconductors, led to the development of two main models such as Hoping model of electrons and small polaron model.

1.4.3.2. Dielectric constant:

Ferrites show high dielectric constant and dispersion of dielectric constant in the frequency range from 20 Hz to 1 GHz. The dielectric properties of ferrites are dependent upon several factors including the method of preparation, chemical composition, grain-size and sintering temperature. A dielectric substance, when subjected to an alternating electric field, the positive and negative charges within the material gets displaced with respect to one another and the system acquires an electric dipole moment. The dipole moment per unit volume is called polarization. Koop's gave a phenomenological theory of dispersion in the dielectric constant.

1.5. APPLICATIONS:

1.5.1. Antenna Core

A winding distributed about the length of a ferrite rod forms an antenna in broadcast radio receivers. The high permeability of the ferrite concentrates the energy in the ferrite, thus increasing the efficiency of reception over that of an air core antenna. The high value of Q of the ferrites gives the antenna a good selectivity. To reduce demagnetizing effects the length –

to-diameter ratio, however the sensitivity of the antenna is increased by increasing the volume of the ferrite rod.

1.5.2. Fly-back transformers and deflection yokes

Large numbers of ferrite cores are used in fly-back transformers for television applications. These cores must have low losses at flux levels up to as high as 1500 gauss the 15.75 kilocycles/sec. the Curie temperature must be high enough so that losses do not rise excessively at the operating temperature. A small ring gap is used to reduce changes caused by the presence of d-c fields.

Cores for deflection yoke in a television picture tube are an example of the use of ferrites of the nickel-zinc-iron or manganese zinc iron variety. The deflection yoke consists of wire coils wound to fit around the neck of a television picture tube. The ferrite cores are molded so that they can be assembled tightly around these coils. These complete structure slips over the neck of a television picture tube. When high frequency current from the tubes of the television set pass through these coils, the electron beam of the picture tube is deflected vertically and horizontally, thus projecting a picture. Because of their high resistivity and the consequent eddy current loss, use of ferrite cores greatly increases the efficiency of the operation. Deflection yokes with a ferrite yokes with a ferrite core.

1.5.3. Inductors

Ferrites are primarily used as inductive components in a large variety of electronic circuits such as low-noise amplifiers, filters, voltage-controlled oscillators, impedance matching networks, for instance. Their recent applications as inductors obey, among other tendencies, to the general trend of miniaturization and integration as ferrite multilayers for passive functional electronics devices. The multilayer technology has become a key technology for mass production of integrated devices; multi layers allow a high degree of integration density. Multi-layer capacitors penetrated the market a few decades ago, while inductors started in the 1980s. The basic components to produce the inductance are a very soft ferrites and a metallic coil.

In addition, to provide a high permeability at the operation frequency, the ferrite film should be prepared by a process compatible with the integrated circuit manufacturing process.

Sputtering provides films with high density, but the composition is sometimes difficult to control with accuracy, and the annealing processes can attain high temperatures. Pulsed laser deposition leads to high- quality films; however, a method involving the preparation of the ferrites film by a combination of sol-gel and spin-coating seems easier and with a lower cost. Layered samples of ferrites with piezoelectric oxides can lead to a new generation of magnetic field sensors. The basis of their performance is the capability of converting magnetic fields into electrical voltages by a two-step process. First, the magnetic field produces a mechanical strain then induces a voltage in the piezoelectric layer. These sensors can provide a high sensitivity, miniature size, and virtually zero power consumption. Sensors for ac and dc magnetic fields, ac and dc electric currents, can be fabricated. Sensors based on nickel ferrites ($Ni_{1-x}Zn_xFe_2O_4$ with x=1-0.5) lead zirconate-titanate ($PbZr_{0.52}Ti_{0.48}O_3$) have shown an excellent performance. Both ferrite and zirconate-titanate films are prepared by tape casting; typically, 11 ferrite layers were combined with 10 piezoelectric layers.

1.5.4. Electromagnetic Interference (EMI) Suppression:

The significance increase in the amount of electronic equipment, such as high-speed digital interfaces, in notebooks, computers, digital cameras, scanners, and so forth, in small areas, has seriously enhanced the possibility of disturbing each other by electromagnetic interferences (EMI). In particular, the fast development of wireless communication has led to interference induced by electric and magnetic fields. Electromagnetic interference can be defined as the degradation in performance of an electronic system caused by an electromagnetic disturbance. The noise from electric devices is usually produced at frequencies higher than circuit signals. To avoid, or at least reduce EMI, suppressors should work as low-pass filter, that is, circuits that block signals with frequencies higher than a given frequency value.

There are several approaches to build EMI suppressors: soft ferrites, ferromagnetic metals, ferromagnetic metal/hexa-ferrite composites, encapsulated magnetic particles and carbon nano-tube composites.

Ferrites components for EMI suppressors have been used for decades. In the recent years, however, there have been special needs for these materials as a consequence of the miniaturization trends, increase in integration density, and increase in higher clock frequency,

especially in communication, computing, and information technologies. Ferrites multilayer components have been developed as a response to these needs, formed essentially by a highly conductive layer embedded in a ferrites monolithic structure, produces by ceramics co-processing technologies. Typically, Ni-Zn ferrites are used for the 20-200 MHz frequency range. Multilayer suppressors behave like a frequency – dependent resistors, at low frequencies, losses in the ferrite are negligible. As frequency increases, losses increase also, and, as ferromagnetic resonance is approached, the inductor behaves as a frequency-independent resistor and no longer as inductor.

1.5.5. Power:

Power applications of ferrites are dominated by the power supplies for a large variety of devices such as computers, all kinds of peripherals, TV and video systems, and all types of small and medium instruments. The main application is in the systems known as switched-mode power supplies (SMPs). In this application, the mains power signal is first rectified, it is then switched as regular pulses (typically rectangular) at a high frequency to feed into a ferrite transformer, and finally it is rectified again to provide the required power to the instrument. An increase power delivery and efficiency can be obtained by increasing the working frequency of the transformer.

A recent approach to increase efficiency of the ferrite cores is based on the decrease of eddy currents, by increasing resistivity. Beside the use of non-conducting additives that locate preferentially on grain boundaries (and limit the inter-grain conductivity), Mn-Zn and Ni-Zn are combined as $Mn_xNi_{0.5-x}Zn_{0.5}Fe_2O_4$ and obtained through a citrate precursor method.

1.5.6. Medical treatment:

Using magnetic jewellery for health is not new. Early civilization recognized that magnetism had restorative properties. Cleopatra frequently adorned herself with magnetic jewels to preserve her youthfulness and health. Magnetic jewellery if often used for general well- being and vitality. It can also be used to treat more specific problems areas in the body. Key acupressure points can be accessed on the wrist, neck and fingers to give relief from pain.

1.5.7. Biosciences:

Magnetic materials in the form of nanoparticles, mainly magnetite (Fe_3O_4), are present in various living organisms and can be used in a number of applications. Magnetic nanoparticles can, of course, be prepared in the laboratory by means of the well-known methods. However, magnetic biogenic particles have better properties than synthetic ones: they are almost perfect crystallographically, and sometimes they possess unusual crystallographic morphologies. Extracellular production of nano meter magnetic particles by various types of bacteria has been described. In many cases, the biogenic particles retain a lipid; layer which makes them very stable and easily biocompatible.

Many biotechnological applications have been developed based on biogenic and synthetic magnetic micro- and nanoparticles. Magnetic nanoparticles have been used to guide radio nuclides to specific tissues. An approach has been developed to directly label a radioisotope with ferrite particles in vivo liver tissue in rats. Therapeutic applications are feasible by further conjugation with other medicals.

In magnetic resonance imaging (MRI), magnetite super-paramagnetic particles are selectively associated with healthy regions of some tissues(liver, for instance); since these particles change the rate of proton decay from the excited to the ground state (which is the basis of MRI), a different , darker contrast is obtained from these healthy regions of tissue.

Thermal energy from hysteresis loss of ferrites can be used in hyperthermia, that is, the heating of specific tissues or organs for treatment of cancer. The addition of magnetic several spinel ferrites (M-Zn, with M=Mn, Co, Fe^{2+} and Fe^{3+} -Mn) are under investigation as well as hexa- ferrites.

Enzymes, oligo-nucleotides, antibodies, and other biologically active compounds can be immobilized, as an important technique used in biotechnology. Such immobilized compounds can be targeted to specific place or can be removed from the system by using an external magnetic field. The compounds can exert their activity on the specific place or tissue or can be used as affinity ligands to trap the cells or target molecules. Magnetic nanoparticles can also be used in a variety of applications: modification, detection, isolation, and study of cells and isolation of biologically active compounds for instance.

CHAPTER II

SYNTHESIS OF FERRITES

2.1 There are different methods of synthesis of ferrites which are reported in literature, some of them are discussed in brief in this chapter.

2.1.1. CERAMIC PROCEDURE:

The most common method of preparing metal oxides and other solid materials is by the ceramic method which involves grinding powders of oxides, carbonates, oxalates or other compounds containing the relevant materials and heating the mixtures at a desired temperature, generally after palletizing the material. Several oxides, sulphides, phosphides have been prepared by this method. Knowledge of phase diagram is helpful in fixing the desired composition and conditions for synthesis. Some caution is necessary in deciding the choice of the container. Platinum, silica and alumina containers are generally used for the synthesis of metal oxides. Most ceramic preparations require relatively high temperatures which are attained by resistance heating.

2.1.2. COMBUSTION SYNTHESIS:

Combustion synthesis or self-propagating high temperature synthesis is a versatile method for the synthesis of a variety of solids. The method makes use of highly exothermic reaction between the reactant to produce a flame due to spontaneous combustion which then yields the desired product or its precursor in finely divided form. Borides, carbides, oxides and other metal derivatives have been prepared by this method. In order that combustion to occur, one has to ensure that the initial mixture of reactant is highly dispersed and contains high mechanical energy. For example, one may add a fuel and oxidizer in preparing oxides by this method, to yield the product or its precursor. Thus one can take a mixture of nitrates (oxidizer) of the desired metal along with fuel (e.g. Hydrazine, Glycine or Urea) in solution, evaporate the solution to dryness and heat the resulting solid to around 423K to obtain spontaneous combustion, yielding an oxides product in fine particulate form. Even if the desired product is not formed just after combustion, the fine particulate nature of the product facilities is formation on the further heating.

2.1.3. SOL- GEL SYNTHESIS:

The sol-gel method has provided a very important means of preparing inorganic oxides. It is a wet chemical method and a multi-step process involving both chemical and physical process such as hydrolysis, polymerization, drying and densification. The name "sol- gel" is given to the process because of the distinctive viscosity increase that occurs at the particular point into the sequence of the step. A sudden increase in viscosity is the common features in sol-gel processing, indicating the onset of gel formation. In the sol-gel process synthesis of inorganic oxides is achieved from inorganic or organo-metallic precursors (generally metal alkoxides). Most of the sol-gel literature deals with synthesis from alkoxides. Ethyl orthosilicate, si(OEt)4 titanium tetra-isopropoxides are typical alkoxides used in sol-gel synthesis.

The important features of sol-gel method are better homogeneity compared to the traditional ceramic method, high purity, lower processing temperature and more uniform phase distribution in multi component system, better size and morphological control, the possibility of preparing new crystalline and non-crystalline materials and lastly easy preparations of thin film and coatings. The sol-gel method is widely used in ceramic technology.

The six important steps involved in the gel synthesis are as follows-

- **HYDROLYSIS**

The process of hydrolysis may start with a mixture of a metal alkoxide and water in a solvent (usually alcohol) at the ambient or a slightly elevated temperature. Acid or base catalyst are added to speed up the reaction.

- **POLYMERISATION**

This step involves condensation of adjacent molecules where in water and alcohols are eliminated and metal oxide linkage are formed. Polymeric networks grow to colloidal dimensions in the liquid (sol) state.

- **GELATION**

In this step a polymeric network, link up to form a three dimensional network throughout, the liquid.

- **DRYING**

Here, water and alcohol are removed at a moderate temperatures (470K), leaving a hydroxylated metal oxide with residual organic content.

- **DEHYDRATION**

This step is carried out between 670K and 1070K to dry out the organic residue and chemically bound water, yielding a glassy metal oxide with up to 20-30% micro porosity.

- **DENSIFICATION**

Temperature in excess of 1270K is used to form dense oxide product.

2.1.4. ELECTROCHEMICAL METHODS:

Electrochemical methods have been employed to advantage for the synthesis of many solid materials. Typical of the materials prepared in this manner are metal borides, silicates, oxides and sulphides. Vanadate spinels of the formula MV_2O_4 as well as tungsten bronzes, A_xWO_3 have been prepared by the electrochemical route. Tungsten bronzes are obtained at cathode when current is passed through two electrodes immersed in a molten solution of alkali metals tungsten A_2WO_4 and WO_3 ; Oxygen is liberated at anode. Blue Mo Bronzes have been prepared by fused salt electrolysis.

2.1.5. CO-PRECIPITATION METHOD:

In this method oxalates of zinc and iron are used as the reactants, these are dissolved in water in the ratio 1:1, the solutions are then mixed and heated to evaporate the water. Oxalates of zinc and iron are gradually precipitated together and resulting fine powder is a solid solution that contains the cations mixed together essentially on an atomic scale. The precipitated solids are filtered off and heated.

$$2Fe\ (COO)_2+Zn(COO)_2\text{----------}\ ZnFe_2O_4+4CO+2CO_2$$

This method has been successfully used for the precipitation of other spinels.

2.1.6. PRECURSOR METHODS:

It was pointed out earlier that diffusion distances for the reacting cations are rather larger in ceramic method. Diffusion distances are markedly reduced to a few angstorms by incorporating the cations in the same solid precursor. A precursor method involves preparation of a compound (precursors) of metals and mixed metals, which yield the desired product of oxides on decomposition. Product obtained is fine, homogeneous in nature, and of high purity. Synthesis of complex by the decomposition of precursor compounds has been known for sometimes. e.g. Thermal decomposition of $LaCo(CN)_6 \cdot H_2O$ and $LaFe(CN)_6 \cdot 6H_2O$ in air readily yield $LaCoO_3$ and $LaFeO_3$ respectively. Ferrite spinels of the general formula MFe_2O_4 (M=Mg, Mn, NI, Co) are prepared by thermal decomposition of acetate precursor of the type $M_3Fe_6(CH_3CoO)_{17}O_3OH \cdot 12C_5H_5N$ chromates of the type MCr_2O_4 are obtained by the decomposition of $(NH_4)M(CrO_4) \cdot 6H_2O$.[1,3]

2.1.7. PRESENT STUDY:

Synthesis of mixed metal ferrites of Mn-Zn and Ni-Zn were carried out by using different chemical compounds with various chemical ligands to generate the precursors which were decomposed utilizing different technique to obtain the desired ferrite products.

CHAPTER III

EXPERIEMENTAL MEASUREMENTS OF Mn-Zn FERRITE

The mixed metal ferrites of Mn-Zn ferrite and Ni-Zn ferrite with general chemical formula $Mn_xZn_{(1-x)}Fe_2O_4$ and $Ni_xZn_{(1-x)}Fe_2O_4$ were synthesized using precursor method and aqeous chemical ligand with different decomposition techniques to obtain the desired ferrite products. The sample obtained were characterized, magnetic and electrical properties were studied for each series which are presented in chapter III first for Mn-Zn ferrite and then in chapter IV for Ni-Zn ferrite.

3.1 The following method was used to prepare Mn-Zn ferrite samples.

3.1.1 BY WET CHEMICAL METHOD:

Manganese Acetate, Zinc Nitrate, Ferric Nitrate were dissolved in minimum quantity of distilled water to obtain aqueous solution of metal ion. To this solution a calculated amount of Succinate hydrazinate ligand solution was added and it was thoroughly mixed to obtain a precursor. The mixture was then kept for drying on a hot plate. The solution dried to a solid mass, which automatically got decomposed into the powdered form and this powders were used for characterization and study of electrical and magnetic properties.

Table 3.1. Amount of compounds taken the synthesis of ferrites.

Sr. No.	Composition	$Mn(CH_3COO)_2.4H_2O$ in g.	$Zn(NO_3)_2.6H_2O$ in g.	$Fe(NO_3)_3.9H_2O$ in g.
1	$Mn_{0.4}Zn_{0.6}Fe_2O_4$	4.9018	8.9240	40.400
2	$Mn_{0.5}Zn_{0.5}Fe_2O_4$	6.1273	7.4368	40.400
3	$Mn_{0.6}Zn_{0.4}Fe_2O_4$	7.3527	5.9494	40.400
4	$Mn_{0.7}Zn_{0.3}Fe_2O_4$	8.5781	4.4620	40.400
5	$Mn_{0.8}Zn_{0.2}Fe_2O_4$	9.8036	2.9747	40.400

3.2. Characterization:

Characterization of materials is an essential part of synthetic study in the development of materials and understanding their compositions, structure etc.

The technique used for characterization of ferrites is

1. Infra- Red Spectroscopy (IR)
2. X-Ray Diffraction Spectroscopy (XRD)
3. Scanning Electron Microscopy (SEM)

3.2.1 Infra -Red Spectroscopy (IR):

It is used in characterization of material as it is quite a versatile tool in the qualitative as well as quantitative analysis of molecular species. In IR spectroscopy identification of various functional groups in unknown substances is carried out through the identification of different covalent bond that are present in the compound and by comparing the absorption seen in an experimental spectrum with the literature of absorptions of various functional groups, it is possible to determine a list of possible identities for the bonds present.

IR absorption spectroscopy helps us to identify the spinel structure. The three typical vibrational bands associated with spinel structure are at (1)600-550cm^{-1} (2)450-385cm^{-1} (3)350-330cm^{-1} for metal-oxygen bands.

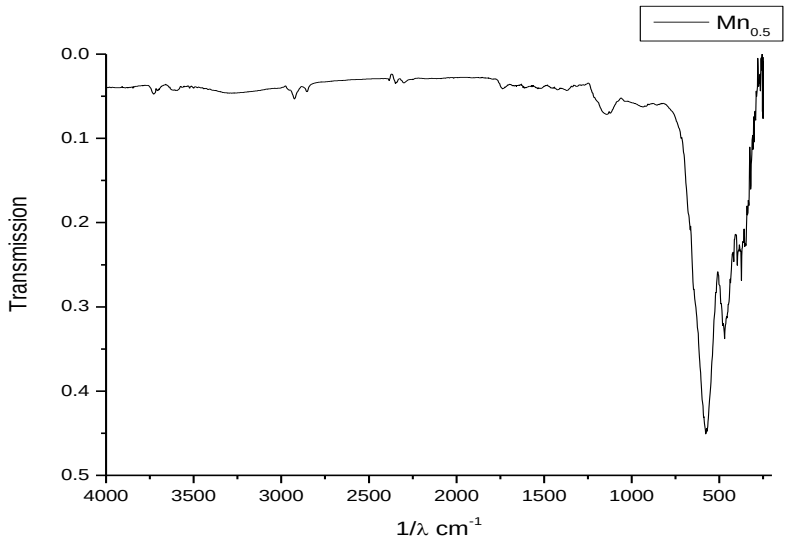

Fig 3.1(a): IR spectrum of $Mn_{0.5}Zn_{0.5}Fe_2O_4$ sample.

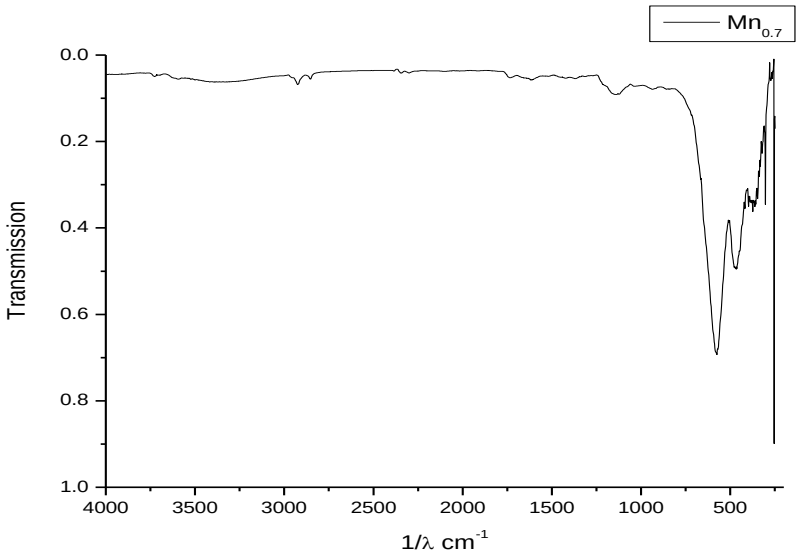

Fig 3.1(b): IR spectrum of $Mn_{0.7}Zn_{0.3}Fe_2O_4$ sample.

3.2.1.1 Results and Discussion

The infrared spectrum of $Mn_{0.5}Zn_{0.5}Fe_2O_4$ and $Mn_{0.7}Zn_{0.3}Fe_2O_4$ ferrite sample is shown in Fig. 3.1(a) and 3.1(b) recorded in the range of 4000-400 cm^{-1}

The IR spectrum of sample show two peaks, one in the range 600-550 cm^{-1} and the other 450-385 cm^{-1} corresponding to:

(a) $Me_T - O - Me_O$ stretching vibration 600-550 cm^{-1}

(b) $Me_O \longleftrightarrow O$ stretching vibration 450-385 cm^{-1}

Here O is oxygen, Me_O is metal in the octahedral site and Me_T in the tetrahedral site. The metal oxygen absorption bands (a) and (b) are pronounced for all spinel structures and essentially for ferrites. For $Mn_{0.5}Zn_{0.5}Fe_2O_4$ sample two bands at 578.14 cm^{-1} and 470.10cm^{-1} and for $Mn_{0.7}Zn_{0.3}Fe_2O_4$ sample two bands at 574.76 cm^{-1} and 461.66 cm^{-1} are observed. Similar patterns were obtained for all the samples. IR spectral data of all the ferrite samples are in agreement with the reported value [4].

3.2.2 X-Ray Diffraction Spectroscopy-

X-Ray powder diffraction (XRD), is an instrumental technique that is used to identify the crystal structure as it is reliable tool for material identification. As the interatomic spacing in the crystal is of the order of 10^{-8} cm, therefore a ray with wavelength of similar order will

give rise to diffraction phenomena. Diffraction provides information about arrangement of atoms in crystals. X-ray powder diffraction of $Mn_xZn_{(1-x)}Fe_2O_4$ samples (with x=0.4, 0.5, 0.6 and 0.8) are illustrated in fig 3.2 .

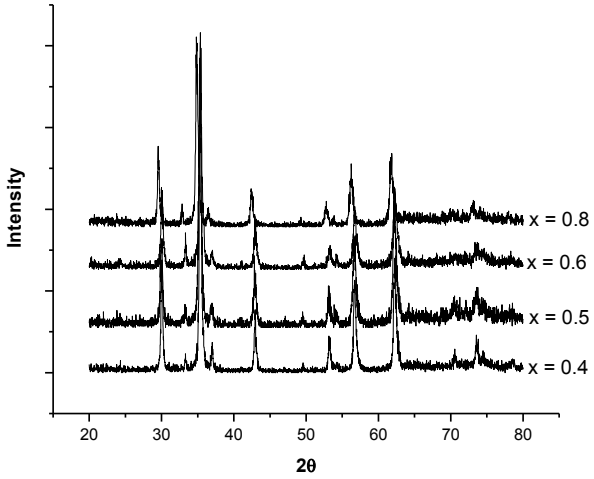

Fig 3.2.: XRD pattern of $Mn_xZn_{(1-x)}Fe_2O_4$ samples .

3.2.2.1 Results and Discussion

The pattern can be clearly identified with single phase cubic spinel structure with no impurity phases as seen from the fig 3.2.

3.2.3. Scanning Electron Microscopy

SEM technique is widely used form of electron microscopy in field of material science. It is an instrument, which is used to observe the morphology of a sample at higher magnification, higher resolution and depth of focus compared to an optical microscope. In SEM an accelerated beam of mono-energetic electron is focused on to the surface of the sample and the small are is scanned by it. Several signals are generated and appropriate ones are collected depending on modes of its operation. The is amplified and made to form a synchronous image of cathode ray tube, the contrast resulting from the morphological changes and the variation of atomic no over the area probed.[5] SEM data was obtained for some samples to observe the surface morphology.

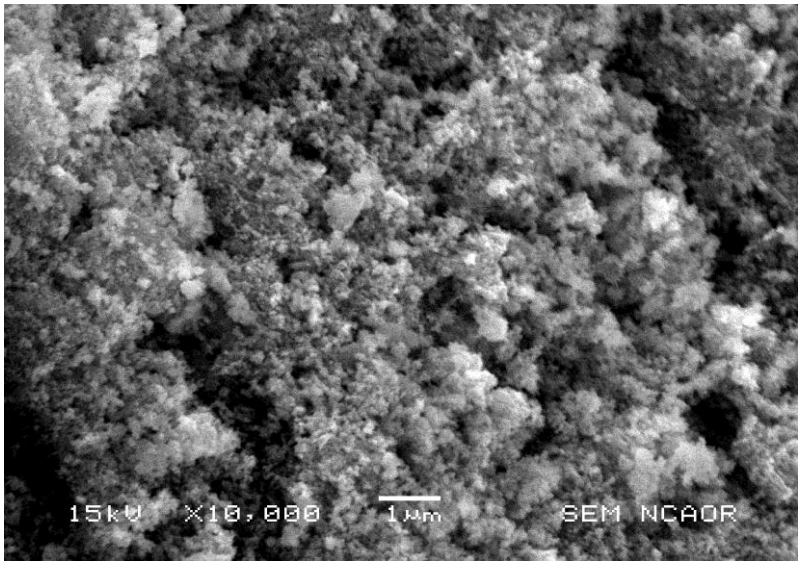

Fig3.3.(a):SEM micrograph of $Mn_{0.5}Zn_{0.5}Fe_2O_4$.

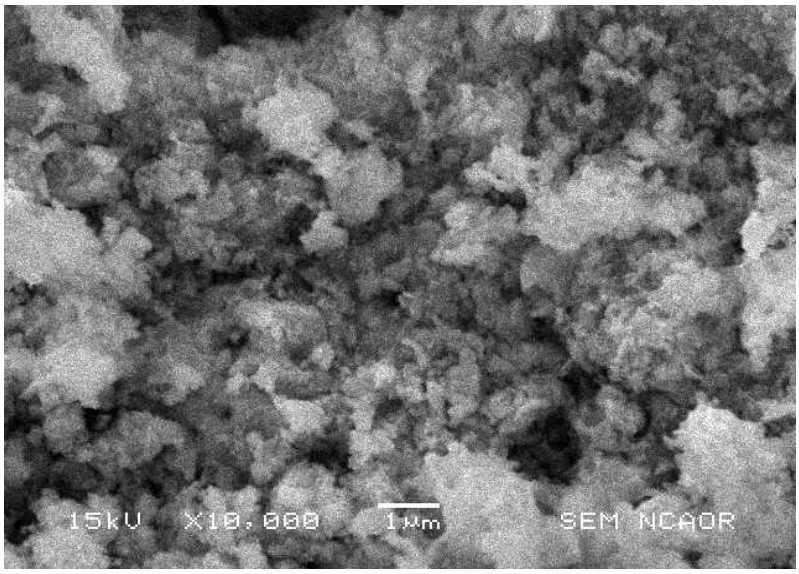

Fig 3.3.(b):SEM micrograph of $Mn_{0.8}Zn_{0.2}Fe_2O_4$.

3.2.3.1. Results and discussion:

It is observed from the SEM micrograph of the samples that the particles are in nano range and has high porosity.

3.3 Physical Properties.

It is always desirable to have knowledge of the physical properties of any solid substance, before it was used for any specific and characteristic applications. The properties associated with solid are density, average particle size, average surface area per unit weight, porosity etc.

In the present study on Mn-Zn ferrites, the investigations were restricted to few of these properties such as inter planar distance, lattice constant, X-ray density and average particle size.

3.3.1. Inter planar distance and Lattice constant from X-ray Diffraction data:

The X-ray data is use to determine interplanar distances and the lattice constants. Due to the random orientation of the crystallites in the sample, a reflection at the particular position is due to a set of atomic planes which are satisfying Braggs condition.

Bragg's equation is given by

$$n\lambda = 2d_{hkl} \sin\theta \qquad 3.1$$

Where d_{hkl} is the interplanar spacing or distance of crystal planes of miller indices (hkl), 'Θ' is the reflection angle, 'λ' is the wavelength of the x-ray radiation and 'n' is the order of reflection.

For a cubic lattice, the interplanar distance $d_{hkl,}$, lattice parameter 'a' and the miller indices (hkl) are related by relation,

$$d_{hkl} = a / (h^2+k^2+l^2)^{1/2} \qquad 3.2$$

thus by using the above relation , the values of lattice constants 'a' were calculated as shown in table 3.2.

3.3.2 X-Ray Density:

X-ray was calculated by using the following relation [6]

$$\rho_x = 8M/Na^3 \qquad 3.3$$

where ρ_x is the x-ray density, '8' represents the no of atoms in unit cell of spinel lattice, 'M' is the molecular weight of ferrite, 'a' is the lattice constant and 'N' is the Avogadro's number.

3.3.3 Particle size using X-ray analysis:

As the particle size decreases the peaks in the XRD patterns get broadened due to the incomplete destructive interference. This broadening caused by the fine crystallites is related to the size of the grains by the Scherer formula.[7]

$$T=0.9\ \lambda/D_p\ \cos\theta \qquad 3.4$$

'T'= Crystallite size, 'λ'=wavelength, 'D_P' FWHM (Full Width Half Measure) 'θ'= reflection angle.

The particle size is an important parameter in the ferrite materials with regards to their applications. By using XRD peak broadening and with help of Scherer formula the particle size values were calculated. The size of Mn-Zn ferrites particles formed were in the nano-meter range. The values are given in Table 3.4.

3.3.3.1 Results and Discussion

Formation of single phase cubic spinel structure of $Mn_{(x)}Zn_{(1-x)}Fe_2O_4$ with x=0.4/0.5/0.6/0.7/0.8 was confirmed with help of XRD patterns obtained for all the samples. As shown in table 3.2. The values of lattice constants 'a' calculated from these were found to increase with increasing Mn concentration and are in excellent agreement with reported values. Similarly the interplanar distance 'd' calculated is also in agreement with the reported values.

The x-ray density calculated as shown in table 3.3 lies in the range of 5.251 g/cc for $Mn_{0.4}Zn_{0.6}Fe_2O_4$ to 5.081 g/cc for $Mn_{0.8}Zn_{0.2}Fe_2O_4$. As the lattice constant increases the x-ray density decreases as it is inversely proportional to lattice constant.

The particle size calculated using the Scherer formula, indicated in Table 3.4. are in the range of 20.4 nm to 41.1nm. This shows that this method gives nano size ferrite particles, which is also confirmed by the SEM micrograph.

Table.3.2 Showing the 'a' values for various $Mn_xZn_{(1-x)}Fe_2O_4$ samples.

Composition	a in A^0
$Mn_{0.4}Zn_{0.6}Fe_2O_4$	8.4219
$Mn_{0.5}Zn_{0.5}Fe_2O_4$	8.4431
$Mn_{0.6}Zn_{0.4}Fe_2O_4$	8.4628
$Mn_{0.7}Zn_{0.3}Fe_2O_4$	8.4704
$Mn_{0.8}Zn_{0.2}Fe_2O_4$	8.4826

Table.3.3 X-ray density for various $Mn_xZn_{(1-x)}Fe_2O_4$ samples.

Concentration of Mn	X-ray density in g/cc
0.4	5.251
0.5	5.206
0.6	5.196
0.7	5.114
0.8	5.081

Table.3.4. Variation of particle size in nm

Concentration of Mn	Particle size in nm
0.4	20.4
0.5	21.9
0.6	34.1
0.7	38.6
0.8	41.1

3.4. Magnetic Properties:

3.4.1. Saturation Magnetization.

Experimental measurement

Powdered samples of $Mn_xZn_{(1-x)}Fe_2O_4$ synthesized were pressed into pellets of the size 1.0 cm in diameter and of thickness ranging between 2mm-3mm under a pressure of 75KN applied for about 3 minutes.

The saturation magnetization measurements of the samples were carried out using a high field hysteresis loop tracer supplied by Magneta, Mumbai India. This instruments works on the principle that the high magnetic field is generated in a solenoid by passing a pulse current of sinusoidal shape. A pickup coil system is kept in the solenoid to detect field and the magnetization signal of a sample placed in the pickup coil. The signals produced are then processed by an electronic system. These transitory signals are digitized by a micro-controller and then sent to computer for plotting a hysteresis loop, which is absorbed on the monitor with calculated values of hysteresis parameters. The applied magnetic field was of 5 KOe. The magnetization sensitivity: was of 10 EMU. The accuracy of measurements was in the

range of 95-100% The calibration of the instrument was carried out using pure nickel as a standard having magnetization 53.34 emu/g.

3.4.1.1 Results and Discussion

The variation of the saturation magnetization with Mn contents for the Mn-Zn ferrite samples of various compositions is given in Table 3.5. It can be observed that the value for saturation magnetization (Ms) increases with increasing Mn ion content. The Ms is minimum for $Mn_{0.4}Zn_{0.6}Fe_2O_4$ i.e. 21.74 emu/g and maximum for $Mn_{0.6}Zn_{0.4}Fe_2O_4$ i.e. 45.17 emu/g. respectively. The hysteresis loss is found to be low for all the samples.

Table 3.5 Variation of saturation magnetization.

Composition	Saturation Magnetization (emu/g)
$Mn_{0.4}Zn_{0.6}Fe_2O_4$	21.74
$Mn_{0.5}Zn_{0.5}Fe_2O_4$	36.52
$Mn_{0.6}Zn_{0.4}Fe_2O_4$	45.17
$Mn_{0.7}Zn_{0.3}Fe_2O_4$	38,91
$Mn_{0.8}Zn_{0.2}Fe_2O_4$	33.11

3.4.2. A.C. Susceptibility:

Curie temperature is one of the most important parameters of ferrites. It is intrinsic property of the spinel ferrites, and depends on method of preparation, sintering temperature, as also on the doping by additives **[8,9]**. The microstructure, porosity and grain size also plays dominant role in deciding the A.C. susceptibility. With respect to their magnetic properties, the ferrimagnetic materials show similarities with those of ferromagnetic. These materials show hysteresis and susceptibility below Curie temperature. A.C. Susceptibility studies explore the existence of multidomain (MD), single domain (SD) and super paramagnetic (SP) particles in the material. From the susceptibility curves **[10-12],** the Curie temperature and domain structure can be determined.

Experimental measurement:

A.C. susceptibility measurements of the unsintered were made using computerized pulse field **A.C.** susceptibility apparatus described by Likhite et al **[13].** The apparatus consists of Helmholtz coil, two pick-up coils, furnace, sample holder, temperature measuring device, control unit, data acquisition system, power supply to run the furnace and PC with related software to execute the run cycle. The Helmholtz coil is powered to produce pulsating magnetic field. To avoid over heating of coils, a glass jacket with water circulation was used. In a typical experiment, the weighed sample was placed in the sample holder, a quartz tube fused at one end, which then was inserted in glass jacket and placed at the centre of the pick-up coil for uniform heating. The data, that is, magnetization (emu/g) as a function of temperature collected by the data acquisition system is directly saved in a file on the PC which simultaneously shows the progress of the experiment by way of a graph on the PC monitor. The temperature of the furnace was maintained by a power supply and was measured by using platinum rhodium thermocouple. It is a regulated digital power supply whose voltage and current are varied automatically by the PID temperature controller output which can be programmed for a set temperature and a set heating rate. The magnetic moments were recorded at various temperatures while, the sample was heated at a preset heating rate. The heating was continued till the magnetization (emu/g) signal reduces to zero. This happens when the Curie temperature is attained.

Table 3.6 Variation of Curie Temperature

Composition	Curie temperature in ^{0}C
$Mn_{0.4}Zn_{0.6}Fe_2O_4$	232
$Mn_{0.5}Zn_{0.5}Fe_2O_4$	257
$Mn_{0.6}Zn_{0.4}Fe_2O_4$	289
$Mn_{0.7}Zn_{0.3}Fe_2O_4$	341
$Mn_{0.8}Zn_{0.2}Fe_2O_4$	384

3.4.2.1 Results and Discussion

The Curie temperature was found to increase with increase in manganese content in the samples $Mn_{0.4}Zn_{0.6}Fe_2O_4$ to $Mn_{0.8}Zn_{0.2}Fe_2O_4$ from 232 ^{0}C to 384 ^{0}C

3.5. Electrical properties:

3.5.1. Resistivity.

Experimental measurement

$Mn_xZn_{(1-x)}Fe_2O_4$ of various composition (x=0.4,0.5,0.6,0.7 and 0.8) samples were pressed into pallets of 10mm in diameter and thickness between 2mm to 3mm under a pressure of 75 KN applied for 3 minutes. The dc resistivity measurements on these samples were then carried out using standard two probe method.

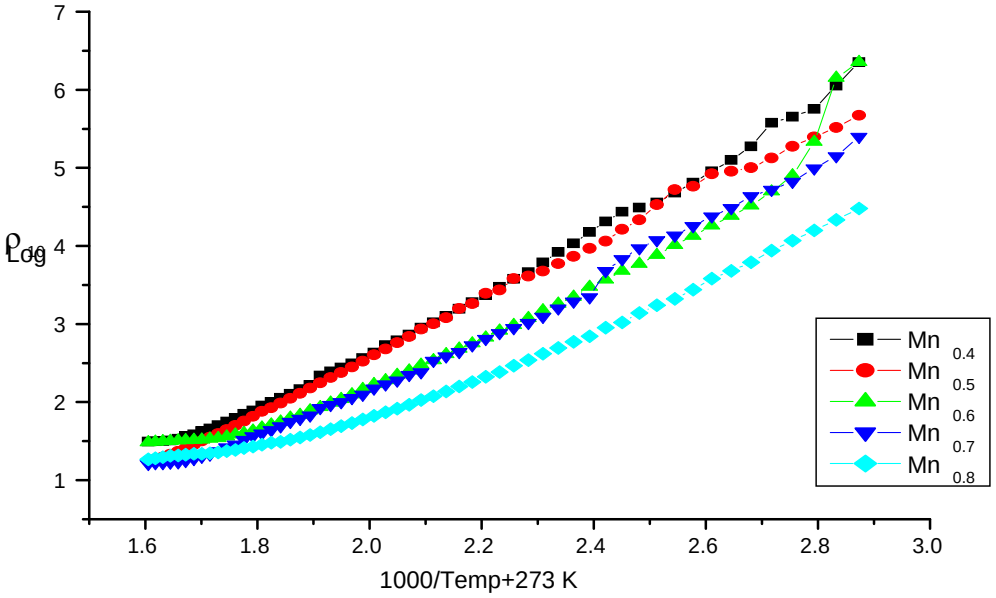

Fig.3.4. Variation of $log_{10}\rho$ with 1000/temp+273 k for $Mn_xZn_{(1-x)}Fe_2O_4$ samples

3.5.1.1. Results and Discussion:

The fig 3.4 shows the graph of $log_{10}\rho$ v/s 1000/T k for the as prepared samples. All the samples show semiconductor behavior wherein initially the conductance is low and it increases with the temperature and also undergoes ferrimagnetic to paramagnetic transition. The curve has two distinct broad parts; initial parts of curve indicating low conductance at lower temperature and later on sharp increase with steep slope when conductance increases or resistivity decreases. The samples show resistivity value in the range 3.6810 X 10^6 ohm cm to 4.7596 X 10^4 ohm cm with low value for $Mn_{0.8}Zn_{0.2}Fe_2O_4$ and high for $Mn_{0.6}Zn_{0.4}Fe_2O_4$ sample synthesized by this method. Electronic conduction mechanisms in ferrites have been studied by many research workers [14] and various models have been proposed; however, the thermally activated hopping model is found to be more appropriate in explaining

quantitatively the electrical behavior of Mn–Zn ferrite. In the hopping process the additional electron on ferrous (Fe^{2+}) ion requires little energy to move to an adjacent (Fe^{3+}) ion on the equivalent lattice sites(B sites). In the presence of the electric field, these extra electron hopping between iron ions give rise to the electrical conduction. Therefore any change in the (Fe^{2+}) ion content in spinel ferrite lattice and/or the distance between them is crucial to the intrinsic resistivity of Mn–Zn ferrite. It is also affected by impurities. The introduction of another cation into the lattice causes a change in the valence distribution on the B sites, then the number of electrons potentially available for transfer will be altered. This is crucial for the conduction mechanism.

3.6. CONCLUSION:

3.6.1. Summary:-

The present study was carried out to synthesize fine particles Mn-Zn mixed metal ferrite material with formula $Mn_xZn_{1-x}Fe_2O_4$ with x= 0.4 0.5, 0.6 0.7 and 0.8 the samples were prepared using the precursor method.

Samples were obtained at low temperature and were confirmed by different methods of characterization such as IR spectral analysis, XRD and SEM analysis

The lattice constant for the samples are in the range of 8.4219 A^0- 8.4826 A^0 . The values are in close agreement with the reported values.

The average particles size calculated using Scherer formula was in the range of 20.4 nm to 41.1 nm.

Saturation magnetization (Ms) values of samples are found increase as manganese content increases but beyond X=0.6 it if found to decrease. The hysteresis losses for the samples are found to be low.

The Curie temperature was found to increase with decrease in non-magnetic Zn content for the samples.

The room temperature dc resistivity is found in the range of 10^4 to $10^6$for the samples of this method. The values of room temperature resistivity are slightly higher than reported values for ceramic method.

Thus This simple precursor method, adopting auto combustion for the synthesis, was found to produce high performance nanoparticle Mn – Zn ferrite materials.

3.6.2. Scope for future work

Further study on magnetic permeability, dielectric constant, thermo electric power and other parameters of ferrites can be carried out. Sintering of the as prepared samples can be done to study the properties of bulk material.

CHAPTER IV

EXPERIEMENTAL MEASUREMENTS OF Ni-Zn FERRITE

4. Study of Nickel Zinc Ferrite:

4.1. Synthesis of $Ni_{(x)}Zn_{(1-x)}Fe_2O_4$ mixed metal ferrites by precursor method.

Stoichiometric amounts of nickel nitrate, iron nitrate and zinc nitrate were taken as per the composition of Ni^{2+}, Zn^{2+} and Fe^{3+} ions mentioned in the table below.

Table 4.1. Amount of compounds taken the synthesis of ferrites.

Samples	Nickel Nitrate in g.	Zinc Nitrate in g.	Iron Nitrate in g.
$Ni_{0.3}Zn_{0.7}Fe_2O_4$	4.3619	10.4114	40.400
$Ni_{0.4}Zn_{0.6}Fe_2O_4$	5.8158	8.9241	40.400
$Ni_{0.5}Zn_{0.5}Fe_2O_4$	7.2697	7.4367	40.400
$Ni_{0.6}Zn_{0.4}Fe_2O_4$	8.7237	5.9494	40.400
$Ni_{0.7}Zn_{0.3}Fe_2O_4$	10.1776	4.4620	40.400

Nickel nitrate, zinc nitrate and iron nitrate were dissolved in minimum quantity of distilled water to obtain aqueous solution of metal ions. To this solution a calculated amount of succinate hydrazinate ligand solution was added and it was thoroughly mixed. The mixture was then kept for drying on a hot plate. The mixture dried to a solid mass which automatically got decomposed into the powder form and these powders were used for characterization and study of electrical and magnetic properties as in the first method.

4.2. Characterization.

Characterisation of material is carried out in order to systematically study the development of materials and to understand their composition, structure, etc. The techniques used for the characterization of ferrite are:

1. Infra Red Spectroscopy (IR)
2. X-ray Diffraction Spectroscopy (XRD)
3. Scanning Electron Microscope

4.2.1. Infra Red Spectroscopy:

Infra Red (IR) Spectroscopy is used in characterization of materials as it is versatile tool in qualitative as well as quantitative analysis of molecular species. In IR spectroscopy identification of various functional groups in unknown substances is carried out through the identification of different covalent bonds that are present in compound and by comparing the absorption seen in an experimental spectrum with the literature of absorption of various functional groups, it is possible to determine a list of possible identities for the bonds present.

IR Spectroscopy allows us to identify the spinel structure. The three typical vibrational bonds associated with spinel structure are at (1) 600-550 cm^{-1} (2) 450-385 cm^{-1} (3) 350-330 cm^{-1} for metal oxygen bonds. IR spectra were obtained for all the samples under investigation confirming formation of spinel ferrite recorded in wavelength range 400 cm^{-1} to 4000 cm^{-1} on Shimadzu FTIR model 8900.The IR absorption spectra obtained for the samples is shown in the fig 4.1 and fig 4.2:

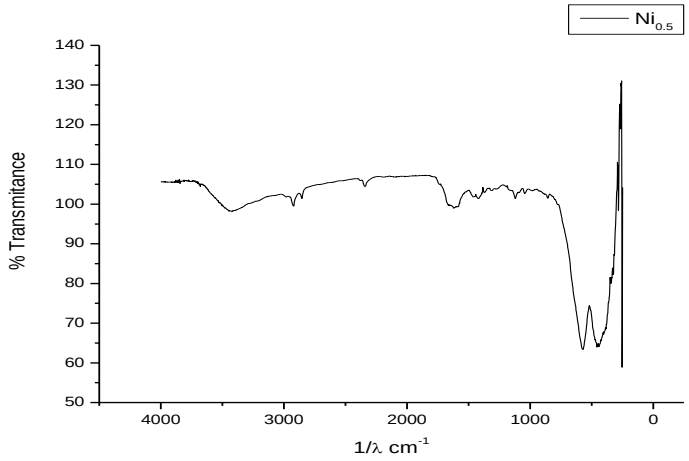

Fig 4.1: IR spectrum of $Ni_{0.5}Zn_{0.5}Fe_2O_4$ sample.

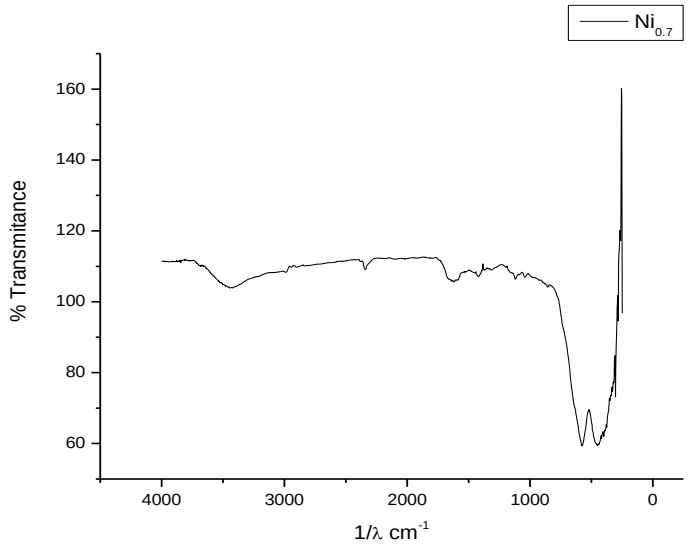

Fig 4.2: IR spectrum of $Ni_{0.7}Zn_{0.3}Fe_2O_4$ sample.

Results and Discussion:-

The infrared spectrum of $Ni_{0.5}Zn_{0.5}Fe_2O_4$ and $Ni_{0.7}Zn_{0.3}Fe_2O_4$ ferrite sample is shown in Fig.4.1 and 4.2. respectively and recorded in the range of 4000-400 cm^{-1}

The IR spectrum of sample show two peaks, one in the range 600-550 cm^{-1} and the other 450-385 cm^{-1} corresponding to:

(c) $Me_T - O - Me_O$ stretching vibration 600-550 cm^{-1}

(d) $Me_O \longleftrightarrow O$ stretching vibration 450-385 cm^{-1}

Here O is oxygen, Me_O is metal in the octahedral site and Me_T in the tetrahedral site. The metal oxygen absorption bands (a) and (b) are pronounced for all spinel structures and essentially for ferrites, which are also seen in the sample. For $Ni_{0.5}Zn_{0.5}Fe_2O_4$ sample two bands are at 570.85 cm^{-1} and 446.35cm^{-1} and for $Ni_{0.7}Zn_{0.3}Fe_2O_4$ sample two bands are at 575.08 cm^{-1} and 445.35 cm^{-1}. Similar patterns were obtained for all the samples. IR spectral data of all the ferrite samples are in agreement with the reported value [15,16].

4.2.2. X-Ray Diffraction Spectroscopy:

X-ray powder diffraction (XRD), is an instrumental technique that is used to identify the crystal structure as it is reliable for material identification. As the interatomic spacing in the crystal is of the order of 10^{-8}cm, therefore a ray with wavelength of similar order will give

rise to diffraction phenomena. X-ray powder diffraction of $Ni_xZn_{(1-x)}Fe_2O_4$ samples (with X=0.3,0.4, 0.5, 0.6 and 0.7) are illustrated in fig.4.3.

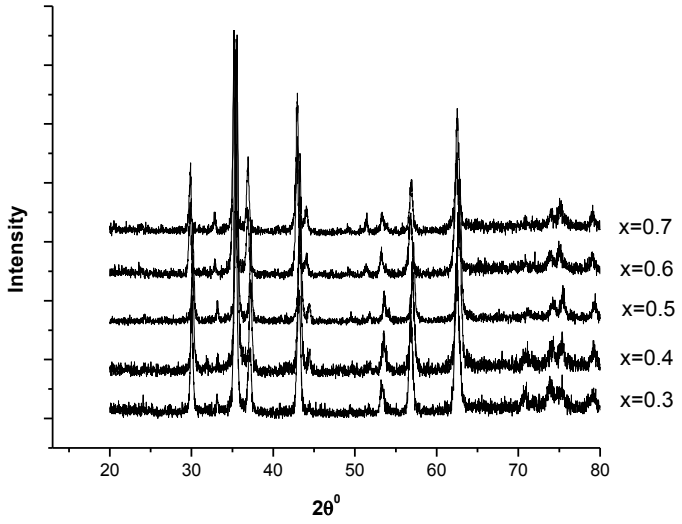

Fig 4.3: XRD pattern of $Ni_xZn_{(1-x)}Fe_2O_4$ samples synthesized by using oxide method.

Results and Discussion:-

The pattern can be clearly identified with single phase cubic spinel structure with no impurity phases as seen from the XRD pattern shown in the above figure.

4.2.3. Scanning Electron Microscopy (SEM)

Scanning Electron Microscopy (SEM) technique is widely used form of electron microscopy in the field of material science. SEM is an instrument, which is used to observe the morphology of a sample at higher magnification, higher resolution and depth of focus compared to an optical microscope. In SEM an accelerated beam of mono-energetic electrons is focused on the surface of the sample and a small area is scanned by it. Several signals are generated and appropriate ones are collected depending on the mode of its operations. The signal is amplified and made to form a synchronous image on the cathode ray tube, the contrast resulting from the morphological changes and the variation of atomic number over the area probed.

SEM data was obtained for some samples to observe the surface morphology.

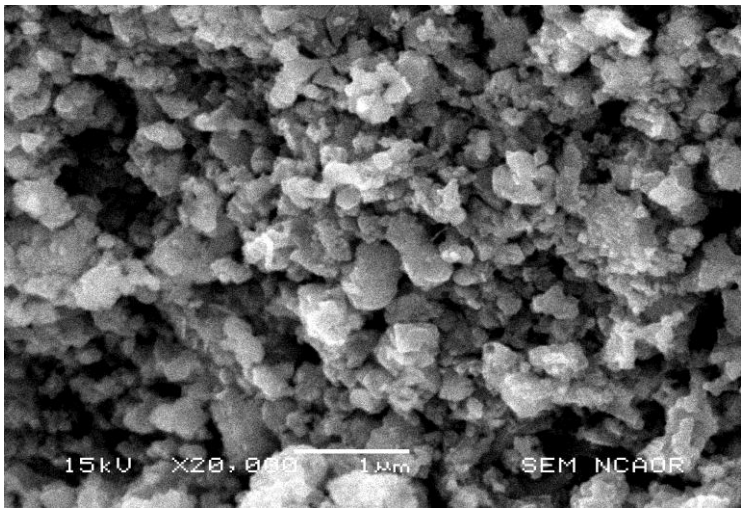

Fig 4.4: SEM micrograph of $Ni_{0.3}Zn_{0.7}Fe_2O_4$.

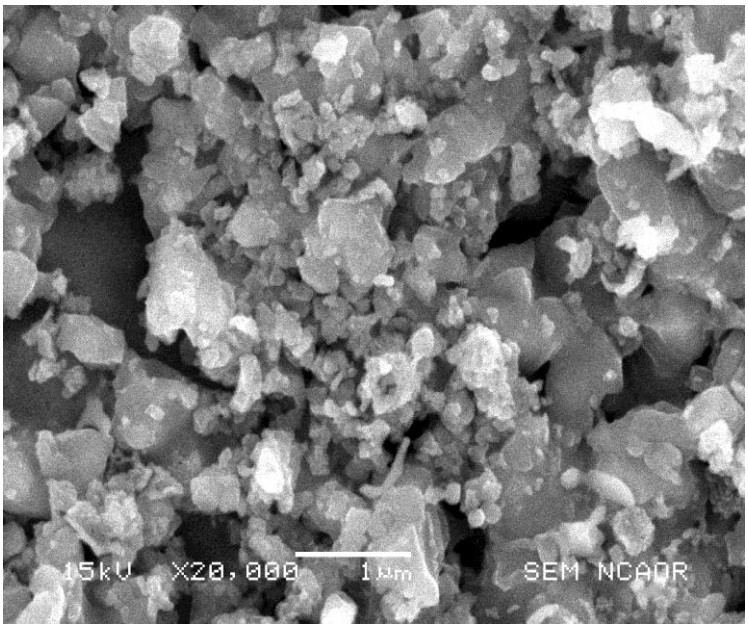

Fig 4.5: SEM micrograph of $Ni_{0.6}Zn_{0.4}Fe_2O_4$.

Results and Discussion:-

As can be seen from the SEM micrograph Fig 4.4 and Fig 4.5 of $Ni_{0.4}Zn_{0.6}Fe_2O_4$ and $Ni_{0.6}Zn_{0.4}Fe_2O_4$ samples obtained from this method that the particles are in nano range and have high porosity.

4.3. Physical Properties.

It is better to have the knowledge of the physical properties of any solid substance, before it is used for any specific and characteristic application. The properties associated with solid are density, average particle size, average surface area per unit weight, porosity, etc.

In the present study on Ni-Zn ferrites, the investigations were restricted to few of these properties such as interplanar distance, lattice constant, X-ray density and average particle size.

4.3.1. Inter Planer Distance and Lattice Constants from X-ray Diffraction Data:

The X-ray data is used to determine interplanar distances and the lattice constants. Due to the random orientation of crystallites in the sample, a reflection at the particular position is due to the set of the atomic planes which are satisfying Bragg's condition.

Bragg's equation is given by:-

$$n\lambda = 2d_{hkl} \sin\theta \qquad (4.1)$$

Where :- 'd'_{hkl} is the interplanar spacing or distance of crystals planes of miller indices (hkl).

'θ' is the reflection angle.

'λ' is wavelength of the X-ray radiation.

'n' is order of reflection.

For a cubic lattice, the interplanar distance d_{hkl}, lattice parameter 'a' and miller indices (hkl) are related by equation :-

$$d_{(hkl)} = a/(h^2+k^2+l^2)^{1/2} \qquad (4.2)$$

thus, by using the above relation (2), the values of lattice constants 'a' were calculated.

4.3.2. X-Ray Density:

The X-ray density was calculated by using the relation[ ] :-

$$\rho_x = 8M/Na^3 \qquad (4.3)$$

where 'ρ_x' is the X-ray density.

'8' represents the number of atoms in a unit cell of spinel lattice.

'M' is the molecular weight of the ferrite.

'a' is the lattice constant.

'N' is the Avogadro's number.

4.3.3 Particle Size Using X-Ray Analysis

As the particle size decreases the peaks in the XRD patterns gets broadened due to the incomplete destructive interference. This broadening caused by the fine crystallites is related to the size of the grains by the Scherer formula [ ].

$$T = 0.9\lambda / D\rho \cos\theta \qquad (4.4)$$

Where :- T=Crystallite size; λ= Wavelength; Dρ= FWHM (Full width half maxima);
θ= reflection angle.

Results and Discussion:-

Formation of single phase cubic spinel structure of $Ni_xZn_{(1-x)}Fe_2O_4$ (X= 0.3,0.4, 0.5, 0.6, and 0.7) samples was confirmed with help of XRD patterns obtained for all the samples. As shown in the table 4.1 and 4.2 the values of lattice constants 'a' calculated from these were found to decrease with increase in Ni concentration. This decrease is attributed to the lower ionic radii of Ni ($0.78A^o$) as compared to Zn ($0.82A^o$) and are in agreement with reported values [17],.

The X-ray density calculated for the samples synthesised using oxide method are shown in table 4.3, it lies in the range of 5.2946 g/cc for $Ni_{0.4}Zn_{0.6}Fe_2O_4$ to 5.3443 g/cc for $Ni_{0.7}Zn_{0.3}Fe_2O_4$ and the X-ray density calculated for the samples synthesised using wet chemical method are shown in table 4.4, and lie in the range of 5.3158 g/cc for $Ni_{0.4}Zn_{0.6}Fe_2O_4$ to 5.3387 g/cc for $Ni_{0.8}Zn_{0.2}Fe_2O_4$ as the lattice constants decreases the X-ray density is found to increase as it is inversely proportional to the lattice constant.

The particle size of samples synthesized using oxide method and wet chemical method is calculated using the Scherer formula, indicated in table 4.5 and 4.6 are in the range from 19.42 nm to 22.58 nm and 22.56 nm to 26.95 nm respectively. This shows that both the method gives nano size ferrite particles, which is also confirmed by the SEM micrograph.

Table 4.1: Variation of lattice constant of $Ni_xZn_{(1-x)}Fe_2O_4$ samples

Samples	Lattice constant "a" in cm.
$Ni_{0.3}Zn_{0.7}Fe_2O_4$	8.4271 X 10^{-8}
$Ni_{0.4}Zn_{0.6}Fe_2O_4$	8.4021 X 10^{-8}
$Ni_{0.5}Zn_{0.5}Fe_2O_4$	8.3963 X 10^{-8}
$Ni_{0.6}Zn_{0.4}Fe_2O_4$	8.3687 X 10^{-8}
$Ni_{0.7}Zn_{0.3}Fe_2O_4$	8.3510 X 10^{-8}

Table 4.2:Variation of X-Ray density for various $Ni_xZn_{(1-x)}Fe_2O_4$ samples

Samples	X-Ray density
$Ni_{0.3}Zn_{0.7}Fe_2O_4$	5.3025
$Ni_{0.4}Zn_{0.6}Fe_2O_4$	5.2816
$Ni_{0.5}Zn_{0.5}Fe_2O_4$	5.3446
$Ni_{0.6}Zn_{0.4}Fe_2O_4$	8.3333
$Ni_{0.7}Zn_{0.3}Fe_2O_4$	5.3426

Table 4.3: Variation of particle size in nm of $Ni_xZn_{(1-x)}Fe_2O_4$ samples

Concentration of Nickel	Particle size in nm
0.3	19.2
0.4	25.6
0.5	29.5
0.6	37. 7
0.7	42.6

4.4. Electrical Properties

The electrical properties are resistivity, dielectric constant thermo electric power etc.

4.4.1. Resistivity:

The resistivity of ferrites is affected by temperature. The diffusion of charge carries from one state to other is possible only when energy exceeds activation energy. The thermal lattice vibration consistently give rise to photons and electrons hop between the pair of states either by absorption or by emission of photons each time in this way transport of charge carries is achieved by hopping process through interaction with photons. On the basis of this the temperature dependence of resistivity of ferrites is given by the relation mention below.

$$\rho = \rho_0 \exp(-\Delta E/kT)$$

Where ρ0 is temperature dependent constant.

ΔE is activation energy. K is Boltzmann constant.

T is absolute temperature.

These factors that differentiate the electrical behaviour of ferrites from that of semiconductors, which led to the development of the two main models such as Hopping Model of electrons and Small Polaron Model.

Experimental Measurements

$Ni_xZn_{(1-x)}Fe_2O_4$ of various composition (X=0.4, 0.5, 0.6, 0.7 and 0.8) samples synthesised using oxide method and wet chemical method were pressed into pallets of 10 mm in diameter and thickness between 2 mm to 3 mm under pressure of 75 KN applied for 3 minutes. The DC resistivity measurements were then carried out using standard two probe method.

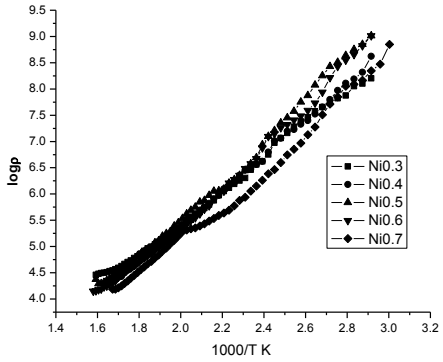

Fig 4.6: Variation of $\log_{10}\rho$ with 1000/T k for $Ni_xZn_{(1-x)}Fe_2O_4$ samples .

Results and Discussion:

The fig 4.6 shows the graph of $\log_{10}\rho$ v/s 1000/Tk for the prepared samples. All the samples show semiconductor behavior wherein initially the conductance is low and it increases with the temperature and also undergoes ferrimagnetic to paramagnetic transition. The curve has two distinct broad parts; initial parts of curve indicating low conductance at lower temperature and later on sharp increase with steep slope when conductance increases or resistivity decreases. The samples show resistivity value in the range 1.3217 X 10^7 ohm cm to 7.4604 X 10^6 ohm cm with low value for $Ni_{0.7}Zn_{0.3}Fe_2O_4$ and high value for $Ni_{0.3}Zn_{0.7}Fe_2O_4$. Electronic conduction mechanisms in ferrites have been studied by many and various models have been proposed; however, the thermally activated hopping model is found to be more appropriate in explaining quantitatively the electrical behavior of Ni–Zn ferrite. In the hopping process the additional electron on ferrous (Fe^{2+}) ion requires little energy to move to an adjacent (Fe^{3+}) ion on the equivalent lattice sites(B sites). In the presence of the electric field, these extra electron hopping between iron ions give rise to the electrical conduction. Therefore any change in the (Fe^{2+}) ion content in spinel ferrite lattice and/or the distance between them is crucial to the intrinsic resistivity of Ni–Zn ferrite. It is also affected by impurities. The introduction of another cation into the lattice causes a change in the valence distribution on the B sites, then the number of electrons potentially available for transfer will be altered. This is crucial for the conduction mechanism.[14]

4.5. Magnetic Properties

The magnetic properties include saturation magnetization, retentivity, coercivity, permeability, susceptibility and Curie temperature.

When the applied field is decreased, magnetization decreases. In multi domain bulk materials, demagnetization occurs primarily via spin rotation through the domain walls. If the demagnetization curve, during the removal of the applied field, does not follow the initial magnetization curve, the material displays hysteresis, which is the lag observed.

Remanance magnetization (Mr) is the magnetization at zero applied field (H=0). The magnetic field applied in the negative direction requires returning the magnetization to zero is the coercive force (Hc).

Experiment Measurement:

4.5.1 Saturation magnetization:

Powder samples of $Ni_xZn_{1-x}Fe_2O_4$(X= 0.3, 0.4, 0.5, 0.6 and 0.7) were pressed into pellets of the size 10 mm diameter of thickness between 2 mm to 3 mm under a pressure of 75 KN applied for 3 minutes. The saturation magnetization and hysteresis loss measurement on the samples were carried out using a high field hysteresis loop tracer, supplied by Magneta, Mumbai.

Table 4.4: Variation of saturation magnetization of $Ni_xZn_{(1-x)}Fe_2O_4$ samples prepared by oxide method.

Concentration	Saturation Magnetization (emu/g)
$Ni_{0.3}Zn_{0.7}Fe_2O_4$	31.64
$Ni_{0.4}Zn_{0.6}Fe_2O_4$	39.28
$Ni_{0.5}Zn_{0.5}Fe_2O_4$	47.86
$Ni_{0.6}Zn_{0.4}Fe_2O_4$	41.16
$Ni_{0.7}Zn_{0.3}Fe_2O_4$	36.31

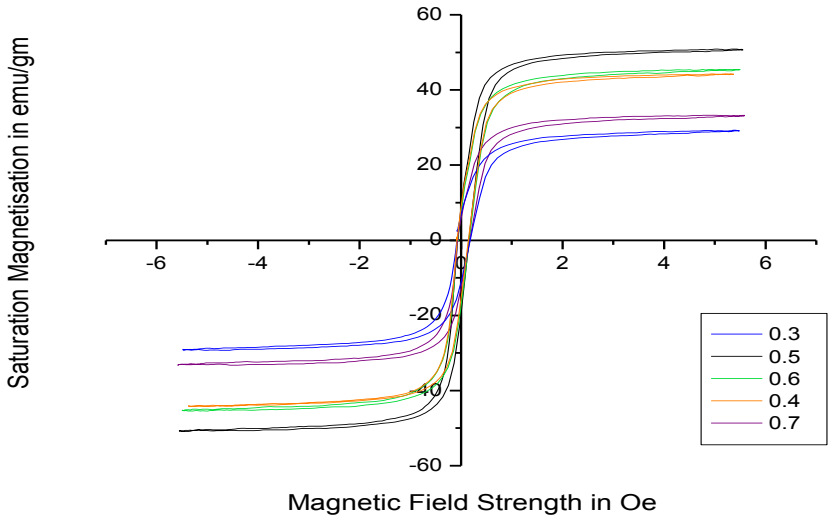

Figure 4.7: Variation of Saturation magnetization

.

Results and Discussion:-

The variation of the saturation magnetization with Ni contents for the Ni – Zn ferrite samples of various compositions is given in Table 4.4. it can be observed that the value for saturation magnetization increases with increasing Ni content upto x= 0.5 with Ms = 47.86 emu/g and then decreases. The hysteresis loss is found to be low for all the samples as can be seen from the graph given in the fig 4.7.

Experimental measurement:

4.5.2. Curie temperature

Curie temperature of $Ni_xZn_{(1-x)}Fe_2O_4$ samples where (X= 0.3, 0.4, 0.5, 0.6 and 0.7) were carried out using the same experimental set up described for Mn Zn ferrite at section 3.4.2 using the instrument supplied by magneta india.

Results and Discussion

The Curie temperature was found to increase with increase in nickel content in the samples $Ni_{0.3}Zn_{0.7}Fe_2O_4$ to $Ni_{0.7}Zn_{0.3}Fe_2O_4$from 204 ^{0}C to 392 ^{0}C

Table 4.5: Variation of Curie temperature of $Ni_xZn_{(1-x)}Fe_2O_4$ samples

Samples	Curie temperature in ^{0}C
$Ni_{0.3}Zn_{0.7}Fe_2O_4$	204
$Ni_{0.4}Zn_{0.6}Fe_2O_4$	247
$Ni_{0.5}Zn_{0.5}Fe_2O_4$	311
$Ni_{0.6}Zn_{0.4}Fe_2O_4$	368
$Ni_{0.7}Zn_{0.3}Fe_2O_4$	392

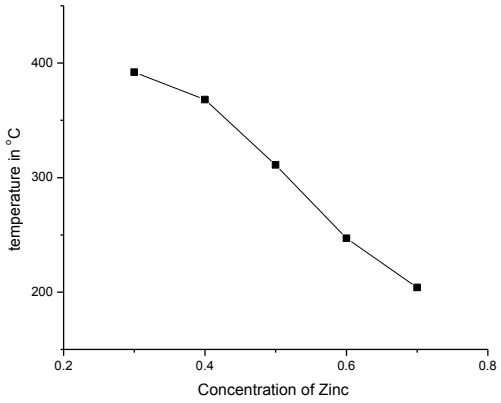

Figure 4.7: Variation of Curie temperature

4.6. CONCLUSION:

4.6.1. Summary:-

The present study was carried out to synthesize fine particles Ni-Zn mixed metal ferrite material with formula $Ni_xZn_{(1-x)}Fe_2O_4$ samples where (X= 0.3, 0.4, 0.5, 0.6 and 0.7) the samples were prepared using the precursor method.

Samples were obtained at low temperature and were confirmed by different methods of characterization such as IR spectral analysis, XRD and SEM analysis

The lattice constant for the samples are in the range of 8.4271 A^0- 8.3510 A^0 . The values are in close agreement with the reported values.

The average particles size calculated using Scherer formula was in the range of 19.2 nm to 42.6 nm.

Saturation magnetization (Ms) values of samples are found increase as nickel content increases up to X=0.5 it is found to decrease thereafter. The hysteresis losses for the samples are found to be low.

The Curie temperature were found to increase with decrease in non-magnetic Zn content for the samples.

The room temperature dc resistivity is found in the range of 10^6 to $10^7$for the samples of this method. The values of room temperature resistivity are slightly higher than reported values for ceramic method.

Thus This simple precursor method, adopting auto combustion for the synthesis, was found to produce high performance nanoparticle NI – Zn ferrite materials.

4.6.2. Scope for future work

Further study on magnetic permeability, dielectric constant, thermo electric power and other parameters of ferrites can be carried out. Sintering of the as prepared samples can be done to study the properties of bulk material.

References:

[1] A. R. West, 'Solid State Chemistry and its Applications', John Wiley and Sons (2007).

[2] www.google.Ferrites.com

[3] C.N.R. Rao and J. Gopalakrishnan, New Directions in Solid State Chemistry, Cambridge University Press, (1986).

[4] A.A. Sattar, H.M. El-Sayed, K.M. El-Shokrofy and M.M. El-Tabey J. Applied Sciences 5 (1) (2005) 162-168.

[5] J. Goldstein, 'Scanning Electron Microscopy and X-ray Microanalysis,' Kluwer Academic Plenum Publishers, (2003).

[6] B. D. Cullity, 'Elements of X-ray Diffraction,' 2nd edition, Addison Wesley (1978).

[7] V. J. Pissurlekar and J. S. Budkuley, Asian J. Chem. 23, 4 (2011), 1677-1679.

[8] A. A. Sattar and K .M. El-Shokrofy J. Phys. IV France 7 Colloq (1997), Cl- 245.

[9] N. Rezlescu, S. Instrate, E. Rezlescu and Luca. J.Phys. Chem. Solid.35,43 (1974).

[10] G. J. Baldha, R.G.Kulkarni, Solid Stat. Commun. 53 (1985)11.

[11] C. Radhakrishnnamurthi, J.Goel. Soc. India 26(9) [1985] 640.

[12] R. V. Uphadhay, G. J. Baldha, R. G. Kulkarni, Mater.Res.Bull.21(1986)1015.

[13] S. D. Likhite, C. Radhakrishnamurthy, Curr. Sci. 35 (1966) 534.

[14] M. I. Klinger and A. A. Samokhvalov, Phys. Status Solidi B 79 (1977) 9.

[15] V. C. Farmer, "The Infrared Spectra of Minerals" ed. V. C. Farmer, Mineralogical Society, London, (1974) 18.

[16] R. Iyer, R. Desai, R. V. Upadhyay, Bull. Mater. Sci., 322, (2009) pp. 141–147.

[17] S.S. Kumbhar , M.A.Mahadik , V.S.Mohite , K.Y.Rajpure , J.H.Kimb, A.V.Moholkar, C.H.Bhosale .J. Magne. Magne. Mater., 363, (2014) 114–120.